A Chain-Intrinsic Fluorescence Study of Orientation–Strain Behavior in Uniaxially Drawn Poly(ethylene terephthalate) Film

B. Clauss[†] **and D. R. Salem***

TRI/Princeton, P.O. Box 625, 601 Prospect Avenue, Princeton, New Jersey 08542

Received April 14, 1995[⊗]

ABSTRACT: The chain-intrinsic fluorescence technique was used to investigate the development of orientation in the noncrystalline phase of PET film during drawing at 90 °C. It was confirmed that orientation develops faster at higher strain rate. In the low draw ratio (precrystallization) regime, the orientation–strain data at high strain rate can be fitted to the affine network model, but at low strain rate, where relaxation effects are substantial, this model is not applicable. We found considerable deviation from the linear stress-optical law: it appears that a stress threshold must be reached before significant orientation takes place and that the threshold value increases with strain rate. Crystallization onset seems to increase the rate of development of orientation at the lower strain rate, probably by providing additional junction points. At both high and low strain rates, however, there eventually occurs an abrupt decrease in the rate of development of orientation (and crystallinity) which coincides with a sharp increase in stress. By comparing our data to some results in the literature on uncrystallizable PEMT, we infer that the slowing of orientation development arises from chain slippage and that the increase in stress largely results from the reinforcing effect of crystallites and an increase in polymer viscosity arising from the interconnection of crystallites.

Introduction

The theoretical background and major features of a new experimental setup for the determination of orientation in the noncrystalline phase of poly(ethylene terephthalate) (PET) have been described in an earlier paper.[1] This technique is based on the excitation of an associated ground state dimer[2,3] (a sandwich of two terephthaloyl moieties of adjacent PET chains) at 334 nm and detection of the emitted fluorescent light at 390 nm. Using polarized incident light and measuring the polarized components of the fluorescent light, one can calculate averages of the orientation distribution function.

It has been shown that the polarized fluorescence at 390 nm can be exclusively attributed to chains in the noncrystalline region.[1–4] A precise side by side alignment of the phenylene rings with a 0.35 nm distance between them is needed for fluorescent emission, and this arrangement is randomly realized in the noncrystalline phase. In crystalline PET, however, fluorescent emission is prevented due to a displaced arrangement of the phenylene rings and a ring separation that is too large (0.4–0.45 nm).

Polarized intrinsic fluorescence must be clearly distinguished from fluorescence methods that incorporate fluorescent probes in the polymer. These probes are not necessarily perfectly aligned with the polymer chain, and the degree of alignment may change during deformation above the glass transition temperature T_g. By using the intrinsic fluorescence of the PET chain, these problems can be avoided and we can therefore expect a more accurate description of the polymer chain orientation in the noncrystalline regions.

Apart from our earlier study,[1] the only work reported in the literature that used the polarized intrinsic fluorescence of PET to determine orientation in the noncrystalline phase was conducted by Hennecke and Fuhrmann.[2,5] However, they investigated the development of orientation during drawing of semicrystalline PET films, whereas the PET films used in most other orientation studies were intially noncrystalline. Until now, therefore, it has not been possible to compare data from the polarized intrinsic fluorescence technique directly with the results from other methods of measuring orientation in the noncrystalline regions. Various studies on strain–orientation behavior of (initially noncrystalline) PET, using methods other than chain-intrinsic fluorescence, have yielded valuable insights. In particular, the extensive work of Bower, Ward, and co-workers[6–13] has indicated that, up to moderate draw ratios, the uniaxial deformation of PET at 80 °C can be adequately described by the affine network model. It is unclear, however, whether this model would be applicable to higher draw temperatures. In the temperature region of 80 °C, PET of "normal" molecular weight appears to be in its most rubberlike state, but at higher temperatures flow type behavior starts to appear, and at low temperatures glassy behavior becomes evident. In the present study, we examine the orientation–strain behavior of PET film drawn at 90 °C, where relaxation effects and strain rate dependence are relatively strong, and we assess the applicability of the rubber-network model in this temperature region. We also investigate noncrystalline orientation development at moderate and high draw ratios where crystallization takes place and where the maximum extensibility of an affine network would be exceeded. For this draw ratio region, we attempt to obtain a clearer notion of the influence of crystallization on the development of orientation in the noncrystalline phase and on the development of stress.

Experimental Section

The amorphous, undrawn PET film ($\bar{M}_n$ = 19 000, i.v. = 0.6) was supplied by Rhône-Poulenc. It was additive-free and of high clarity, with a density of 1339 kg/m^3. The amorphous film was uniaxially deformed to various draw ratios on an Instron tensile tester at a draw temperature of 90 °C and at nominal strain rates of 0.01 and 0.56 s^{-1}. Immediately after reaching 90 °C, the film was drawn at the selected extension rate. At the end of the drawing, the sample was air-quenched

* To whom correspondence should be addressed.
† Present address: Institut für Textilchemie, Körschtalstrasse 26, 73770 Denkendorf, Germany.
⊗ Abstract published in *Advance ACS Abstracts,* November 1, 1995.

0024-9297/95/2228-8328$09.00/0

by opening the furnace door. The specimen geometry of the undrawn film was such that the deformation mode was essentially simple extension (see ref 1). The setup and procedure used for determining the second moment of the (noncrystalline) orientation distribution $\langle P_2(\cos\theta)\rangle_{a/fl}$ from the polarized intrinsic fluorescence of the PET film have been described in detail elsewhere.[1]

Results and Discussion

Low to Moderate Draw Ratios. Several studies of orientation in the noncrystalline phase of hot-drawn PET[6-13] suggest that the affine rubber-network model, which has been developed to describe the deformation of cross-linked polymers in the rubber elastic state, can also describe the deformation of PET above its T_g. The rubber elasticity theory assumes a permanently cross-linked system of polymer chains having a certain number of rotatable segments between cross-link points. The Gaussian approximation assumes further that the distance r between cross-link points is much less than the chain length, which is given by the number of rotatable segments N multiplied by their length. Another important assumption of this model is that the deformation of the network is affine, which means that the measured macroscopic draw ratio is equivalent to the deformation on the molecular level. In the case of PET, there are no chemical cross-links, but one can imagine that chain entanglements may also act as cross-links. This Gaussian network model leads to a simple equation, relating the second moment of the orientation function to the draw ratio λ:

$$\langle P_2(\cos\theta)\rangle = \frac{1}{5N}(\lambda^2 - 1/\lambda) \qquad (1)$$

For PET films hot-drawn at 80 °C, Nobbs, Bower, and Ward[8] found a linear relationship between molecular orientation in the noncrystalline regions (determined by the incorporated fluorescence probe method) and $\lambda^2 - 1/\lambda$. It was suggested that the polymer can be modeled as a rubber network with 5.6 freely jointed links between cross-link points, when uniaxially drawn (or drawn and shrunk) at 80 °C, provided the draw ratio is less than 2.5. At higher draw ratios strain-induced crystallization occurred. An attempt to model the orientation behavior after the onset of crystallization is given in another paper by Nobbs et al.,[10] where it is assumed that the affine rubber model changes to a pseudo-affine scheme when chains whose end-to-end vectors were originally in the draw direction become fully extended. This occurs when $\lambda = N^{1/2}$, being the theoretical limit for the rubber-network model.[14] Calculations based on this modified model result in a slightly lower N value of 5.12 for the rubber region and a reasonable fit for the data points in the draw ratio region above 2.5. However, Nobbs et al. pointed out that there might be a combination of various mechanisms whose net effect on the orientation averages is similar to that predicted by this model.

We will now report our attempts to fit our orientation data from intrinsic fluorescence to the Gaussian rubber-network model. Our films were drawn at 90 °C; that is, at a temperature 10 °C higher than the drawing temperature in the studies discussed above.[6-13]

At first sight, the Gaussian rubber-network model seems to provide reasonable fits to our data up to moderate draw ratios (Figure 1), suggesting the following interpretations: (1) We have a rubberlike entanglement network with 4.4 and 14 rotatable segments between cross-link points for strain rates of 0.56 s^{-1} and 0.01 s^{-1}, respectively; (2) higher strain rates allow less time for relaxation processes and therefore result in higher apparent cross-link densities or lower values of N.

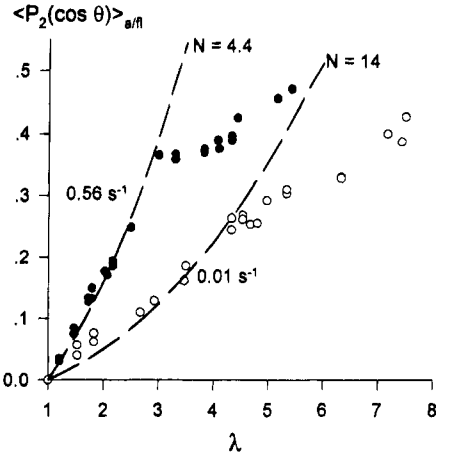

Figure 1. Orientation development of noncrystalline chains at two strain rates, and theoretical curves for Gaussian network model with 4.4 and 14 rotatable segments between cross-link points.

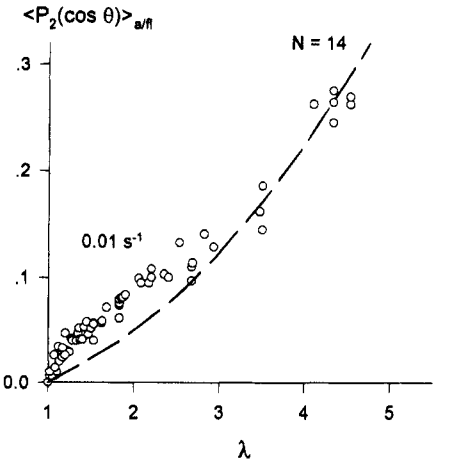

Figure 2. Orientation development of noncrystalline chains at the lower strain rate, and the curve predicted by the Gaussian network model.

However, a closer examination of the data indicates that, for the strain rate of 0.01 s^{-1}, the fit is relatively poor at draw ratios less than about 2.5. We therefore collected additional data at draw ratios <3 in order to determine the shape of the curve more exactly. The complete set of data is shown in Figure 2, from which it is apparent that the Gaussian rubber model does not adequately describe the orientation–strain behavior at the lower strain rate. Similarly, Figure 3 shows that, contrary to the predictions of the Gaussian rubber model, the orientation function is not linearly related to $\lambda^2 - 1/\lambda$. In fact, all forms of the affine network theory predict orientation–strain curves with increasing slopes, whereas Figure 2 clearly displays a decreasing slope up to a draw ratio of about 3.

At the strain rate of 0.56 s^{-1}, the situation is less clear. The rubber-network model seems to fit the data well up to a draw ratio of about 3 (Figures 1 and 4), but this is beyond the theoretical limit of $\lambda = N^{1/2}$. It is possible that the Gaussian approximation is causing an underestimation of the value of N. In any case the strains being considered are high enough, and the values of N small enough, that significant error may be

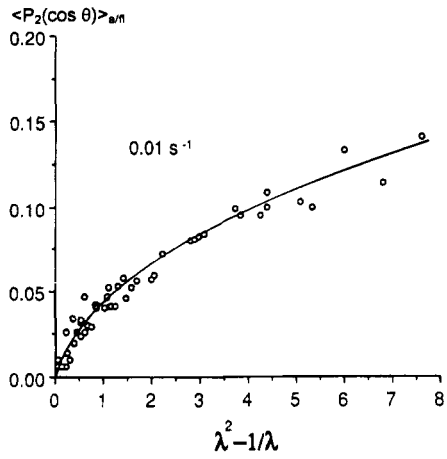

Figure 3. Noncrystalline orientation versus $\lambda^2 - 1/\lambda$ for low strain rate drawing, up to $\lambda \simeq 3$ (the precrystallization regime).

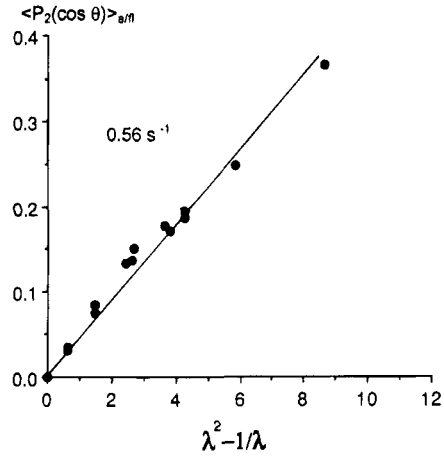

Figure 4. Noncrystalline orientation versus $\lambda^2 - 1/\lambda$ for high strain rate drawing, up to $\lambda \simeq 3$.

arising from the use of this approximation, and we have therefore examined the predictions of the more exact treatment, given by the first three terms of the series expansion of the inverse Langevin function:[14,15]

$$\langle P_2(\cos\theta)\rangle = \frac{1}{5N}(\lambda^2 - 1/\lambda) + \frac{1}{25N^2}(\lambda^4 + \lambda/3 - 4/3\lambda^2) + \frac{1}{35N3}(\lambda^6 + 3\lambda^3/5 - 8/5\lambda^3) \quad (2)$$

The consequences of using eq 2 rather than eq 1 are that the value of N is now 5.2 instead of 4.4, and the theoretical curve no longer fits the data so well once λ exceeds $N^{1/2}$ (Figure 5).

Another way to check the applicability of the rubber-network model is to examine stress–strain curves. The Gaussian network theory predicts the following relationship between true stress and draw ratio:

$$\sigma_{true} = nkT(\lambda^2 - 1/\lambda) \quad (3)$$

where n is the number of cross-links per unit volume, k is Boltzmann's constant, and T is absolute temperature. A plot of σ_{true} versus $\lambda^2 - 1/\lambda$ should result in a linear relationship if the model is applicable.

Bearing in mind that onset of crystallization occurs at values of $\lambda^2 - 1/\lambda$ of 4.4 and 9.9 for strain rates 0.56 s^{-1} and 0.01 s^{-1}, respectively,[1] it can be seen from Figure 6 that these plots by no means give linear curves in the precrystallization regime; and using the inverse Langevin function to predict network stress does not provide better agreement.

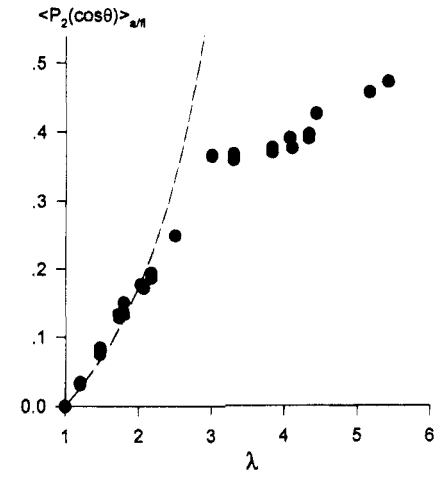

Figure 5. Noncrystalline orientation vs draw ratio at a strain rate of 0.56 s^{-1}, and the curve predicted by the inverse Langevin form of the network model with $N = 5.2$.

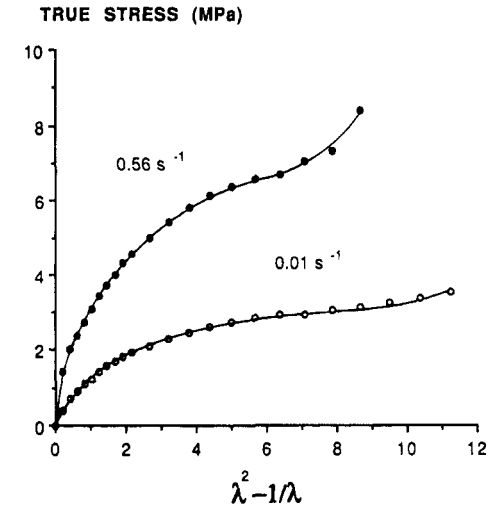

Figure 6. True stress versus $\lambda^2 - 1/\lambda$ at two strain rates.

Thus, for the high strain rate, the orientation data in the precrystallization regime seem to support the rubber-network model, whereas the stress data contradict it. A similar discrepancy between orientation–strain and stress–strain data was noted by Bower et al. for drawing at 80 °C.[12] For the lower strain rate, neither the orientation nor the stress data can be adequately described by the rubber-network model.

We are inclined to interpret these results as follows. When relaxation effects are small, due to low temperature and/or high strain rate, the rubber-network model can adequately describe the strain-dependent orientation of PET molecules prior to crystallization. But when the combination of strain rate and draw temperature results in substantial orientational relaxation during drawing, this model is no longer applicable. The fact that the development of stress cannot be described by the rubber deformation scheme even at the high strain rate could imply that the stress relaxation time constant is smaller than the time constant for orientational relaxation. It can certainly be seen from Figure 7 that the linear stress-optical law is not applicable to the deformation of PET film under either of the drawing conditions we have examined. There have been various reports in the literature[16–19] of deviations from the linear stress-optical law when amorphous polymers are

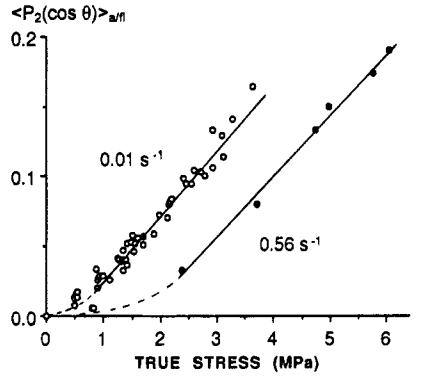

Figure 7. Noncrystalline orientation versus true stress at two strain rates, for films drawn in the precrystallization regime.

stretched at temperatures greater than, but close to, T_g. Muller and Pesce[19] showed that, in the approximate range T_g to T_g + 20 °C, the relaxation of birefringence in polystyrene and polycarbonate is a much slower process than the relaxation of stress and that the initial increase in stress results in almost no increase in orientation. The phenomenon of delayed orientation onset becomes more pronounced as temperatures decrease toward T_g and vanishes at temperatures $>T_g$ + 20 °C. Our data indicate that the delay in orientation onset also increases with strain rate (Figure 7). Muller and Pesce suggested that the total tensile stress is made up of two contributions: an entropic stress related to the chain orientation and a nonentropic stress which is strongly temperature dependent. Possible molecular origins of the nonentropic stress were not discussed.

Brown and Windle[20–23] have developed a deformation model for the rubber and glass states in which the strain resulting from an applied tensile stress is resolved into two components: an orientational component, associated with the alignment of individual chain segments; and a translational, or extensional, component associated with the unraveling of chains without any net increase in orientation. Interestingly, this model predicts that a threshold value of stress must be obtained before significant orientation develops and that this value increases with strain rate.[22] Also, Brown and Windle's model yields orientation–strain relationships qualitatively similar to that found for the PET film drawn at 0.01 s^{-1} in the present study. So far, however, we have been unable to obtain acceptable quantitative fitting of our data to this model.

Moderate to High Draw Ratios and the Influence of Crystallization. In previous publications we reported that crystallization during constant extension rate drawing of PET film occurs in two regimes: a low stress regime in which crystallinity increases relatively fast (regime 1), followed by a high stress regime in which crystallinity increases slowly (regime 2).[1,23] We also reported that the onset of crystallization seems to coincide with the inflection point in the true stress vs strain relationship.[23] Although the latter observation was from PET film drawn in pure shear, we have also found it to apply to film drawn in uniaxial extension—the deformation conditions of the present study. Figure 8 shows a direct comparison of the development of true stress and (noncrystalline) orientation as functions of draw ratio λ for the strain rate of 0.01 s^{-1}, in which three regimes can be distinguished. It is interesting to notice that the inflection point in the orientation–strain curve, as well as in the stress–strain curve, occurs at a draw

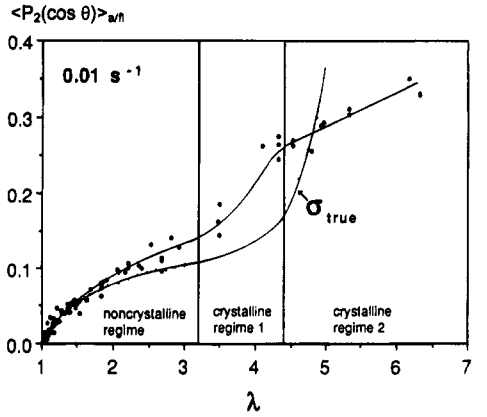

Figure 8. Development of noncrystalline orientation as a function of draw ratio compared with the development of true stress (arbitrary scale).

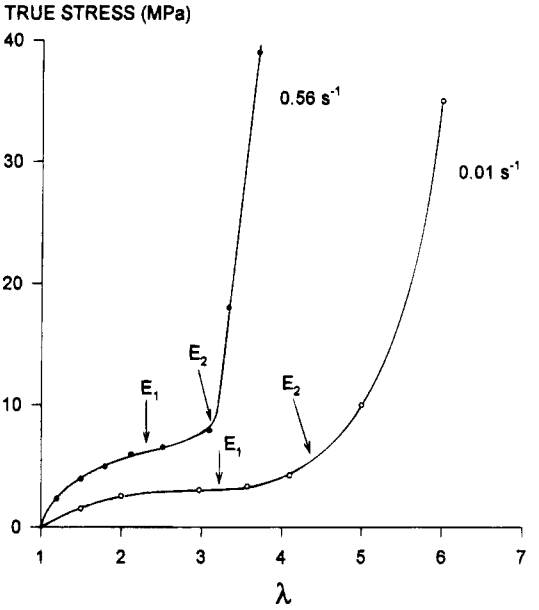

Figure 9. True stress versus draw ratio at two strain rates. The onset of crystallization, E_1, and the onset of regime 2 crystallization, E_2, are indicated.

ratio of about 3.2, which is the point at which crystallization begins.[1] It can be argued that, in crystallization regime 1, additional junction points provided by crystallites promote more efficient orientation of chains. Eventually, however, we believe that the crystallites take over from entanglements as the predominant junction points (regime 2 crystallization), forming a network which results in a substantial increase in the stress required to deform the polymer. This is accompanied by a sharply reduced rate of development of orientation in the noncrystalline phase, which we will discuss in more detail later.

For the strain rate of 0.56 s^{-1}, the inflection point in the stress–strain curve occurs at a draw ratio of about 2.2 (Figure 9), corresponding to the onset of crystallization (see ref 1). However, the shape of the orientation–strain curve at this strain rate is somewhat open to interpretation. In Figures 1 and 5, we drew curves with an increasing slope in the precrystallization regime, in accordance with the affine deformation scheme. It is possible, however, to assign a slightly decreasing slope with an inflection point at $\lambda \simeq 2.2$ (Figure 10). Clearly there is insufficient resolution in the orientation–strain data at 0.56 s^{-1} to distinguish decisively between these alternatives.

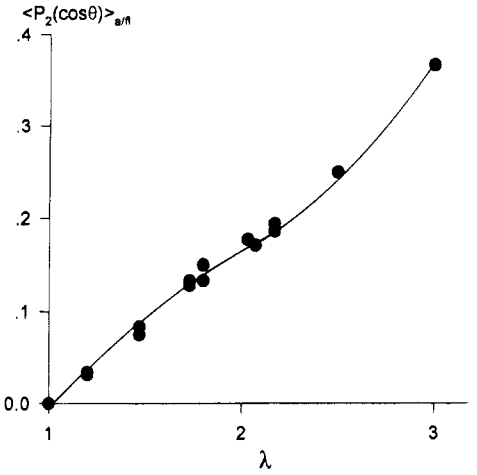

Figure 10. Noncrystalline orientation versus draw ratio at the strain rate of 0.56 s^{-1}.

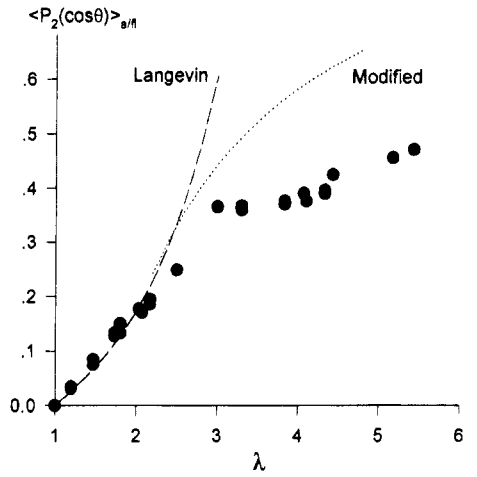

Figure 11. Comparison of the modified rubber-network model[9] with experimental data at the strain rate of 0.56 s^{-1} ($N = 5.2$).

To model orientation development of an affine network when draw ratio exceeds $N^{1/2}$, Nobbs and Bower proposed that chains which become fully extended be considered to rotate as rigid rods (pseudo-affine scheme) while the end-to-end vectors of chains which are not fully extended continue to rotate and extend affinely.[9] This leads to the following expression for values of $\lambda > N^{1/2}$:

$$\langle P_2(\cos\theta)\rangle = \frac{128N^{1/2}}{175\lambda} \quad (4)$$

Nobbs and Bower pointed out that, in reality, once chains are fully extended, either departure from affine deformation must take place or chains must break or slip at the cross-link points, reducing N. Also, this approach does not explicitly take into account the influence of crystallization. Nevertheless, the model provided an adequate fit to orientation–strain data of PET film drawn at 80 °C[10] and also showed rough agreement with the orientation–strain behavior of uncrystallizable poly(ethylene methyl terephthalate) (PEMT) film drawn at 65 °C. (Since the T_g of PEMT is 15–20 °C lower than PET, these drawing temperatures are approximately equivalent.)

Using the 0.56 s^{-1} strain rate as the example, it can be seen from Figure 11 that the modified rubber scheme of Nobbs and Bower does not fit our 90 °C orientation–strain data at high draw ratios. It is interesting to notice that the model showed a similar overestimation of the orientation at high draw ratios when applied to the deformation of PEMT at 70 °C.[24] Indeed, in the high draw ratio region, the rate of development of orientation decreases to about zero when PEMT is drawn at this temperature. It can therefore be inferred that, in the presence or absence of crystallization, the rate of orientation development drops abrupty at high draw ratios, especially when the drawing temperature significantly exceeds T_g. The major influence of crystallization appears to be on the stress–strain relationship. For drawing of uncrystallizable PEMT film at 70 °C, it was found that a linear (shrinkage) stress vs birefringence relationship holds to the highest birefringences.[24] This clearly indicates an abrupt decrease in the rate of development of stress at high draw ratios, which is in sharp contrast to the rapid increase in stress observed for PET. We suggest that at high draw ratios the deformation behaviors of PET and PEMT are both characterized by considerable chain slippage, resulting in inefficient chain orientation. In the case of PET, however, crystallites provide reinforcement and possibly a network structure in which translational slippage between "tie-segment blocks"[25] of crystallites could occur. Indeed, the fact that the upturn in stress occurs at a characteristic volume fraction crystallinity, independent of strain rate,[1,23] is suggestive of a percolation transition, and we are investigating this possibility further. The evidence to date certainly indicates that the steep rise in stress at high draw ratios can be predominantly attributed to reaching a critical level of crystallinity.

Conclusions

Based on our present study, using a draw temperature of 90 °C, and based on the previous studies of Bower, Ward, and co-workers,[10] using a draw temperature of 80 °C, it appears that the orientation–strain behavior of PET film in the precrystallization regime can be predicted by the affine network model provided that the combination of strain rate and temperature does not result in substantial orientational relaxation during drawing. Thus, at a draw temperature of 90 °C and a strain rate of 0.56 s^{-1}, the orientation–strain data fit the rubber-network theory up to $N^{1/2}$ and yield a value of 5.2 rotatable segments between (entanglement) cross-links. At a strain rate of 0.01 s^{-1}, however, the orientation–strain curve has a decreasing slope up to a draw ratio of about 3, differing from the rubber-network theory which predicts an increasing slope.

The stress–strain data do not conform to the rubber-network model at either strain rate, and there is appreciable deviation from the linear stress-optical law. It appears that a critical stress must be reached before significant orientation takes place and that the critical stress increases with strain rate. A similar phenomenon in amorphous polymers deformed near T_g has been observed by others,[16–19] and it implies that the total tensile stress is made up of an entropic and a nonentropic component.

The onset of crystallization coincides with the inflection point in the stress–strain curves, and stress increases slowly throughout the early stages of crystallization. In this crystallization regime, "noncrystalline orientation" continues to increase rapidly during high strain-rate deformation, and during low strain-rate deformation it significantly accelerates, possibly due to the provision of crystallite junction points. At higher

draw ratios, however (when volume fraction crystallinity has reached about 0.15), there occurs an abrupt decrease in the gradients of the orientation–strain and the crystallinity–strain curves together with a sharp increase in the gradient of the stress–strain curve. Since studies on the deformation of uncrystallizable PEMT[24] indicate that the rate of both orientation and stress development decrease abruptly at high draw ratios (probably due to chain slippage), we infer that the increase in stress displayed by PET is mainly attributable to the reinforcing effect of crystallites and an increase in polymer viscosity arising from the interconnection of crystallites.

Acknowledgment. This study was undertaken in connection with the TRI project "Structure and Properties of Poly(ethylene terephthalate) Film", supported by a group of Corporate TRI Participants. The authors are grateful to Dennis W. Briant and Lei Zhang of the TRI staff for assistance with the experimental work, and to Dr. William Merrill for helpful discussions.

References and Notes

(1) Clauss, B.; Salem, D. R. *Polymer* **1992**, *33*, 3193.
(2) Hennecke, M.; Furhmann, J. *Makromol. Chem. Macromol. Symp.* **1986**, *5*, 181.
(3) Sonnenschein, M. F.; Roland, C. M. *Polymer* **1990**, *31*, 2023.
(4) Hemker, D. J.; Frank, C. W.; Thomas, J. W. *Polymer* **1988**, *29*, 437.
(5) Hennecke, M.; Kud, A.; Kurz, K.; Furhmann, J. *Colloid Polym. Sci.* **1987**, *265*, 674.
(6) Cunningham, A.; Ward, I. M.; Willis, H. A.; Zichy, V. *Polymer* **1974**, *15*, 749.
(7) Purvis, J.; Bower, D. I. *J. Polym. Sci., Polym. Phys. Ed.* **1976**, *14*, 1461.
(8) Nobbs, J. H.; Bower, D. I.; Ward, I. M. *Polymer* **1976**, *17*, 25.
(9) Nobbs, J. H.; Bower, D. I. *Polymer* **1978**, *19*, 1100.
(10) Nobbs, J. H.; Bower, D. I.; Ward, I. M. *J. Polym. Sci., Polym. Phys. Ed.* **1979**, *17*, 259.
(11) Rietsch, F.; Duckett, R. A.; Ward, I. M. *Polymer* **1979**, *20*, 1133.
(12) Bower, D. I.; Jarvis, D. A.; Ward, I. M. *J. Polym. Sci., Polym. Phys. Ed.* **1986**, *24*, 1459.
(13) Nobbs, J. H.; Ward, I. M. Polarized Fluorescence in Oriented Polymers. Chapter 4 in *Polymer Photophysics*; Phillips, D., Ed.; Chapman & Hall: London, 1984.
(14) Treleor, L. R. G. *Trans. Faraday Soc.* **1954**, *50*, 881.
(15) Roe, R. J.; Krigbaum, W. R. J. *J. Appl. Phys.* **1964**, *35*, 2215.
(16) Retting, W. *Colloid Polym. Sci.* **1983**, *23*, 835.
(17) Inoue, T.; Okamoto, H.; Osaki, K. *Macromolecules* **1991**, *24*, 5670.
(18) Read, B. E. *Polym. Eng. Sci.* **1983**, *23*, 835.
(19) Muller, R.; Pesce, J. J. *Polymer* **1994**, *35*, 734.
(20) Brown, D. J.; Windle, A. H. *J. Mater. Sci.* **1984**, *19*, 1997.
(21) Brown, D. J.; Windle, A. H. *J. Mater. Sci.* **1984**, *19*, 2013.
(22) Brown, D. J.; Windle, A. H. *J. Mater. Sci.* **1984**, *19*, 2039.
(23) Salem, D. R. *Polymer* **1992**, *33*, 3182.
(24) O'Neill, M. A.; Duckett, R. A.; Ward, I. M. *Polymer* **1988**, *29*, 54.
(25) Buckley, C. P.; Salem, D. R. *Polymer* **1987**, *28*, 69.

MA950511J